International Research Symposium
Rajarata University of Sri Lanka

IRSyRUSl 2015

Fluorescent Extended Aromatic Molecular Materials: Nitrogen Heterosuperbenzene Family

Buddhie SL[1]*, Sylvia MD

School of Chemistry, University of Dublin, Trinity College, Dublin 2, Ireland

ABSTRACT

*Different types of extended aromatic molecular materials exhibit unique molecular structures and the resulting extraordinary electronic, thermal and mechanical properties make them promising candidates for future electronics and composite materials. The electrical and optoelectronic properties of such molecules rely heavily on extended π–conjugation. Herein reports which promise the establishment of a family of heterosuperbenzenes with intrinsic carbon-nitrogen frameworks. Oxidative cyclodehydrogenation is a significant process in the formation of planar heteropolyaromatic graphenes such as N-HSB (**1**), N-⅔HSB (**2**) and N-½HSB (**3**). These graphenes result from the $FeCl_3$ catalyzed oxidative cyclodehydrogenation of 1,2-dipyrimidyl-3,4,5,6-tetra-(4-tert-butylphenyl)benzene. The extended aromaticity and enhanced planarity of **1**, **2** and **3** confer interesting spectroscopic properties on them. In the context of LED applications, the systematic replacement of carbon atoms with electronegative nitrogen atoms enhances the carrier transport of the system. There is a paucity of processable forms of electron-acceptor materials with desired thermal stability. N-heterosuperbenzenes (**1**, **2** and **3**) offer a significant advance in this regard.*

*In conclusion, the essential steps in the formation of intrinsically nitrogen-doped graphite nanostructures in a controlled and systematic manner have been proven. The presence of N atoms has rendered overall electron-accepting properties to **1** compared to its all-C analogue. The emission studies on **1**, **2** and **3** suggest that the optoelectronic properties of this emerging heterosuperbenzene family will be promising because their quantum yields and life-times. Synthetic control of the extent and position of N doping such as demonstrated here allows molecular tuning of the optoelectronic properties of the resultant material and provides the potential for ligand-based functionality.*

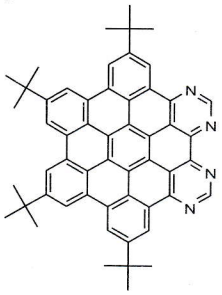

(1)

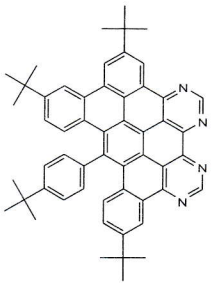

(2)

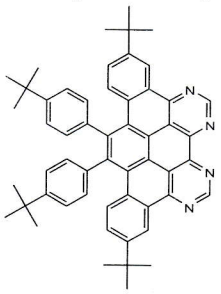

(3)

KEYWORDS: *Aggregation, N-HSB, Oxidative cyclodehydrogenation and Photophysical properties*

[1] * Corresponding Author: Buddhie SL: buddhieslankage@gmail.com

1 Introduction

The early discoveries of the electrical and optoelectronic properties of polycyclic aromatic hydrocarbons (PAHs) have now led to promising applications in the field of organic electronics (Müllen *et al.*, 2007). The electrical and optoelectronic properties of such molecules rely heavily on extended π–conjugation. In this area, organic chemists have pursued various π–conjugation systems as active components for electronic and optoelectronic devices such as light-emitting diodes (LEDs), solar cells and many others molecular electronic devices (Grimsdale *et al.*, 2009). The key physical processes for these applications are the transport and recombination of electrical charges. In particular, the mobility of the charge carrier in the solid-state materials is one of the most important parameter that determines the device performance (Aleshin *et al.*, 1997).

Depending on their size and shape and the favourable overlap of π–orbitals in adjacent molecules these materials possess the ability to form ordered columnar mesophases with high charge carrier mobilities along the columnar axis. This makes them suitable as semiconducting materials (Müller and Müllen, 2007). Hexa-*peri*-hexabenzocoronene (HBC) exhibits one of the highest intrinsic charge carrier mobilities for a discotic material (van de Craats and Warman, 2001). The variation of the periphery, topology, size and shape of a HBC has a distinct impact on its electronic properties and its self-assembling behaviour.

Therefore, it is possible to change the periphery, size and shape of a PAH through substitution of both the ring atoms and their R groups resulting in various PAHs that exhibits unique properties, which will be discussed below.

1.2 Statement of Problem

Generally PAHs with R=H show extremely low solubility in most common organic solvents such as toluene, chloroform etc. This insolubility leads not only for problems when attempting to fully characterise them, but also increases the difficulty of thin film or device fabrication.

1.3 Objective/s of the Study

The introduction of nitrogen atoms and *tert*-butyl groups confers to the nitrogen heterosuperbenzenes the dual advantages of ligand functionality and increased solubility compared to their all-carbon analogues (Draper *et al.*, 2004). In the context of LED applications, the systematic replacement of carbon atoms with electronegative nitrogen atoms enhances the carrier transport of the system. There is a paucity of processable forms of electron-acceptor materials with desired thermal stability. N-heterosuperbenzenes (**1**, **2** and **3**) offer a significant advance in this regard.

1.4 Review of Literature

Distinctly different types of graphitic forms exhibit unique properties which have fascinated the scientific community over the last two decades. Their unique molecular structures and the resulting extraordinary electronic, thermal and mechanical properties make them promising candidates for future electronics and composite materials (Rojas *et al.*, 2008). The electrical and optoelectronic properties of such molecules rely heavily on extended π–conjugation. Müllen *et al.* have developed a route to a series of predefined all-carbon superbenzenes *via* the cyclodehydrogenation of polyphenylene precursors (Watson *et al.*, 2001).

2 Methodology

2.1 Materials

Flash chromatography was performed using silica gel as the stationary phase. All other chemicals were obtained from commercial sources unless otherwise stated.

Nuclear magnetic resonance data were recorded on Bruker DPX 400 and Bruker Avance II 600

spectrometers in $CDCl_3$. Both solvents were standardized with respect to TMS. UV-Vis absorption spectra were recorded on a Shimadzu UV-2401PC. Emission spectra were recorded on a Varian Fluorescence Cary Eclipse spectrophotometer. Electrospray mass spectra (ESI-MS) were obtained on a Micromass LCT Electrospray Mass Spectrometer. The single-crystal analysed on a Brüker SMART APEX CCD diffractometer using graphite monochromised Mo-K_α (λ=0.71073 Å) radiation at the temperature range 298–120 and 23K.

2.2 Synthesis

Carbon polyphenylene precursors are usually generated by the cyclotrimerization (Hyatt, 1991) of phenyl-substituted ethynes, or the Diels-Alder [2+4] cycloaddition of the same with tetraphenylcyclopentadienone (Ogliaruso *et al.*, 1965).

To achieve N-doped polyphenylene modify the established synthetic protocol (Ogliaruso *et al.*, 1965) by incorporating pyrimidine substituents into the alkyne. Di-(pyrimid-3,5-yl)acetylene and 2,3,4,5-tetra-(4-*tert*-butylphenyl)cyclopentadienone were synthesized *via* a Sonogashira coupling reaction and a two-fold Knoevenagel condensation reaction, respectively. The final step in the formation of **1** is the synthesis of the polyphenylene precursor **4** (Scheme 1) *via* the Diels-Alder [2+4] cycloaddition (Ogliaruso *et al.*, 1965) of phenyl-substituted ethynes and tetraphenylcyclopentadienone (Draper *et al.*, 2002).

Intramolecular cyclodehydrogenation of an N-doped hexaarylbenzene (N-HAB) derivative is the key and final step responsible for the 'planarisation' of the N-HAB to furnish a rigid structure (Scheme1).

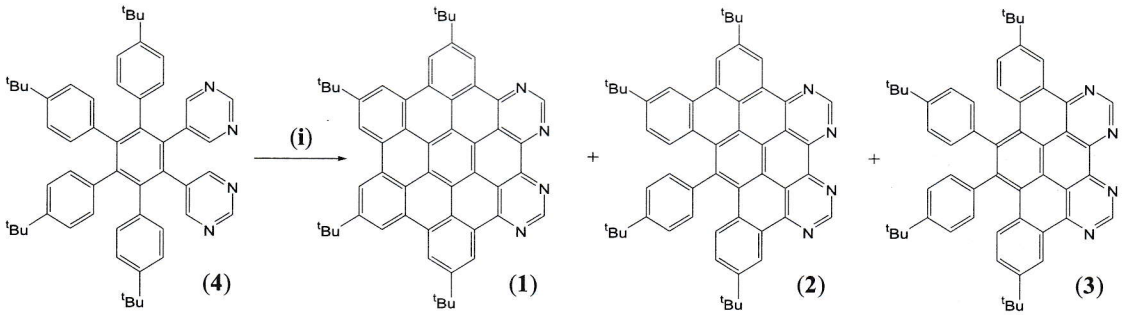

Scheme 1. The synthesis of varied nitrogen-heterosuperbenzenes N-HSB (**1**), N-⅔HSB (**2**) and N-½HSB (**3**) generated by varying degree of planarity *via* intramolecular oxidative cyclodehydrogenation of oligophenelyene precursor (**4**) using (i) $AlCl_3$, $CuCl_2$ and CS_2.

3 Results and Discussion

3.1 Synthesis of N-heterosuperbenzenes 1, 2 and 3

N-HSB (**1**) was obtained *via* oxidative cyclodehydrogenation of **4** using $AlCl_3$ and $CuCl_2$ (46% yield). The cyclodehydrogenation of **4** is lower-yielding than that of the all-carbon polyphenylene precursors and the reason is the formation of several products. Typically all-carbon systems give rise to the fully-cyclised product in over 90% yield (Fogel *et al.*, 2007 and Iyer *et al.*, 1997). In the cyclodehydrogenation of **4**, products **2** and **3** as well as the fully cyclised product **1** (N-HSB, six C–C bond fusions) were identified. When the nitrogen atoms are incorporated into the hexaphenylbenzene precursor (**4**), the fully cyclised product **1** is co-synthesised with partially-cyclised products **2** (N-⅔HSB, four C–C bond fusions) (23% yield) and **3** (N-½HSB, three C–C bond fusions) (20% yield).

3.2 Characterisation

The formation of **1**, **2** and **3** were characterised with the aid of mass spectrometry, elemental analysis,

^{1}H, ^{13}C NMR and 135° DEPT spectroscopy, ^{1}H-^{1}H COSY, ^{13}C-^{1}H COSY (HMQC), IR, UV-Vis absorption and fluorescence spectroscopy. **1** and **2** were further characterised by X-ray crystallography (Lankage, 2010). The melting points of **1**, **2** and **3** were >360 °C.

Mass spectral data of **1** [calculated for $C_{54}H_{47}N_4$, $(M+H)^+$ *m/z* 751.3801; found, 751.2167], **2** [calculated for $C_{54}H_{51}N_4$, $(M+H)^+$ *m/z* 755.4114; found, 755.4104.] and **3** [calculated for $C_{54}H_{53}N_4$, $(M+H)^+$ *m/z* 757.4270; found, 757.4282] were found in toluene.

Figure 1 shows the ^{1}H NMR spectra of **1**, **2** and **3**. The ^{1}H NMR spectra of **1** and **3** is simplified by the presence of a C_2 axis of symmetry running through the molecule as shown in (Figure 1-a and 1-c). ^{1}H NMR spectra of **1** and **3** show two sets of aliphatic signals integrating for 18 hydrogen atoms each, corresponding to the two pairs of equivalent *tert*-butyl protons (Figure 1-a and 1-c). Aromatic region of ^{1}H NMR spectra of **1** shows five signals, each integrating for two hydrogen atoms (Figure 1-a) and **3** shows six signals, 1-4 H's integrating for two hydrogen atoms and 5-6 H's for four hydrogen atoms (Figure 1-c). These results were consistent with the literature values (Draper *et al.*, 2002 and Gregg *et al.*, 2005).

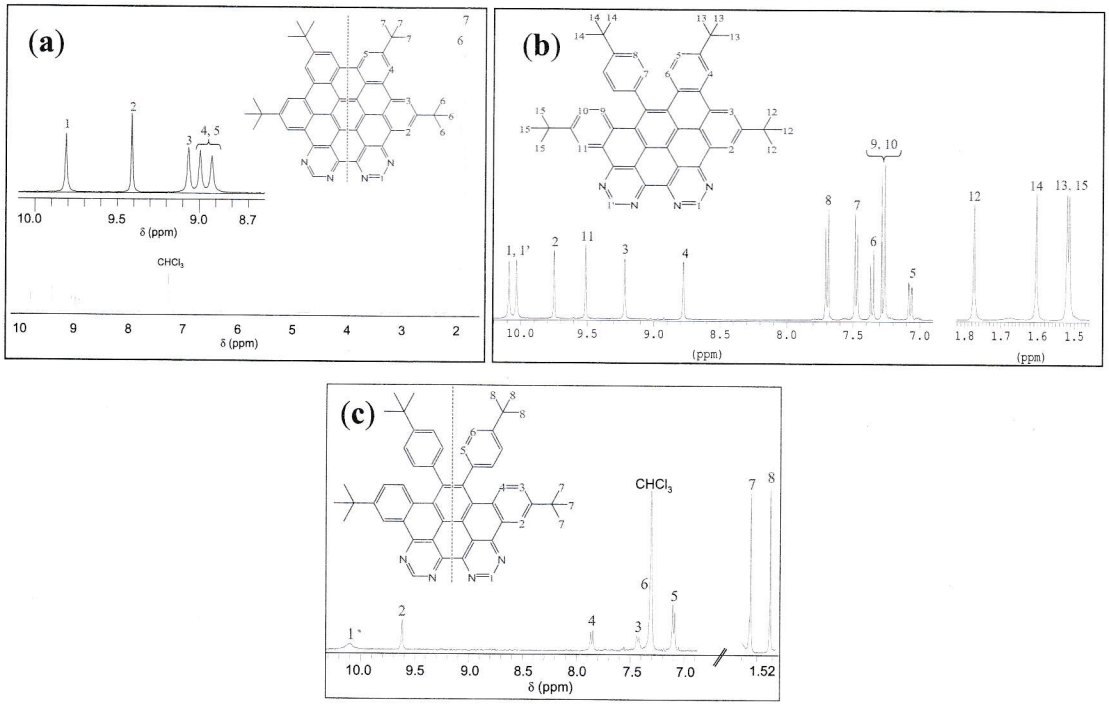

Figure 1. The ^{1}H NMR spectra of (a) N-HSB (**1**), (b) N-⅔HSB (**2**) and (c) N-½HSB (**3**) in $CDCl_3$ at RT, 400 MHz. Note: aromatic regions and aliphatic regions are not drawn on the same scale.

Compound **2** comprises ten fused aromatic rings and one "uncyclised" aryl ring, which can rotate between the partially fused aryl rings. The uncyclised aryl ring can rotate freely because of twisting of the partially fused rings above and below the plane (crystal structure of **2**, Figure 3-a). The presence of this unique ring reduces the size of the aromatic platform compared to **1** and reduces the symmetry. Collectively, 12 aromatic signals are observed in the aromatic region of the ^{1}H NMR spectrum of **2**, integrating for 14 hydrogen atoms. The well-resolved coupling information from ^{1}H NMR, ^{1}H-^{1}H COSY, ^{13}C-^{1}H COSY and NOE spectra permitted the complete assignment of the aromatic and aliphatic proton signals (Figure 1-b). The aromatic signals at lowest field (δ 10.16 and δ 10.10) are assigned to the two hydrogen atoms located between the pyrimidine nitrogens (H1 and H1') and the other four singlets between δ 8.7-9.8 are attributed to the four hydrogens (H2-4) and H11 located on the fused aryl rings (Figure 1-b). The aryl ring that remains uncyclised gives rise to two doublets at δ 7.51 (H7) and δ 7.71 (H8), each integrating for two protons. The ^{1}H NMR spectrum also shows four aliphatic signals for the four sets of *tert*-butyl protons at δ 1.78 (*tert*-butyls of (12) "cyclised" aryl ring),

δ 1.61 (*tert*-butyls of (14) "uncyclised" aryl ring) and δ 1.53 and 1.52 (*tert*-butyls of (13 and 15) "half cyclised" aryl rings), with the latter two signals being almost coincident. These four aliphatic signals each integrate for 9 protons (Figure 1-b). The integration, coupling patterns and chemical shifts of these aromatic signals confirm that four C–C bond fusions have occurred at the pyrimidine-end of the molecule.

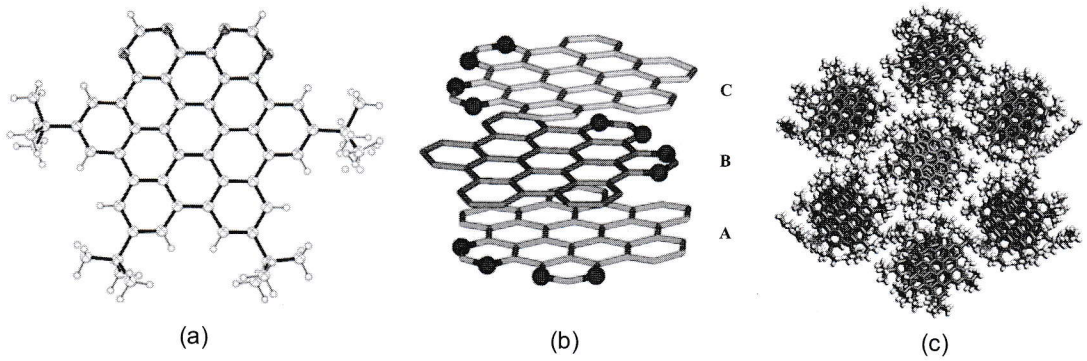

Figure 2. (a) The synchrotron single crystal structure of N-HSB·⅓$CHCl_3$·⅓H_2O (**1**), (b) the pictorial representation of helical ABCABC packing arrangement of the molecules and (c) packing arrangement along *a* axis.

Crystals suitable for synchrotron single-crystal structure analysis were obtained by slow evaporation of a solution mixture of **1** in chloroform/methanol at room temperature. **1** crystallises in the common space group $P2_12_12_1$ with three molecules of **1**, one chloroform molecule and a water molecule in the asymmetric unit (Figure 2-a). In the crystal structure, **1** exists in dimers, stabilised by $\pi\cdots\pi$ interactions measuring approximately 3.7 Å. The remarkable differences in the $\pi\cdots\pi$ stacking of these systems due to changes in peripheral organic substituents have been observed in the literature (Wu *et al.*, 2004).

Molecule **1** is packed in an **ABCABC** columnar stacking arrangement (Figure 2-b) with each column surrounded by six other columns (Figure 2-c). Figure 2-b displays the pictorial representation of the helical arrangement of **1** (*tert*-butyl groups have been removed for easy visualisation). Molecule **B** is rotated 143° from molecule **A** in the columnar stack. Molecule **C** is rotated 153° from **B** and the underlying molecule **A** is rotated by a further 64° from **C**. The molecules of **1** are held together by numerous N···H and N···O intermolecular interactions along with the $\pi\cdots\pi$ interactions. The interactions of N···O and N···H between **1** and solvent molecules are the most significant and strong interactions that were exhibited in the supramolecular network. These results support the observation of solution aggregation in the spectroscopic data.

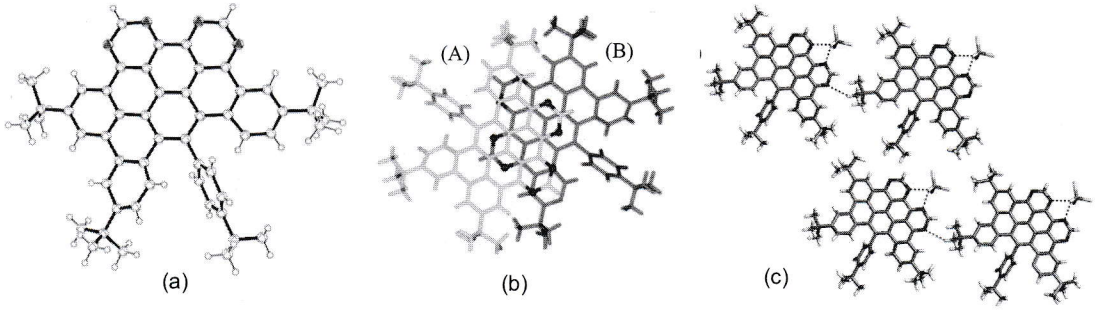

Figure 3. (a) The single crystal X-ray structure of N-⅔HSB·⅓$CHCl_3$ (**2**) (disorder has been removed for clarity), (b) view from above the plane of a dimer (AB) and (c) packing arrangement: intra-layer interactions in the assembly.

Compound **2** crystallises in the common space group P1 with one molecule in the asymmetric unit. The

crystal structure is highly disordered due to the free aryl ring rotation and twisting of the adjacent partially-fused aryl rings (above and below the plane) (Figure 3-a).

Compound **2** comprises ten fused rings and this twisted aromatic platform promotes dimer formation (ABAB packing) due to $\pi\cdots\pi$ interactions (3.41 Å) (Figure 3-b). Also the benzene rings of the planarised portions are offset from each other so that the centre of each six-membered ring is precisely superimposed on a carbon atom in the underlying molecule (Figure 3-b). This behaviour is observed in the ideal crystal structure of graphite known as Bernal stacking (Ebbesen, 1997). These dimers are arranged in a head-to-tail manner, aligning the free aryl rings opposite to each other (Figure 3-b).

The molecular self-assembly of **2** is further held together by N···H interactions with chloroform molecules and very weak interactions in between molecules (Figure 3-c) The most significant N···H interactions are between **2** and chloroform forming a layered self-assembly. The interlayer (A and B) $\pi\cdots\pi$ interactions form a sandwich-type molecular self-assembly in the crystal packing arrangement. The distance between the sandwich-type (AB AB) double layers is approximately 4.80 Å. These results support the aggregation observed in solution spectroscopic data of **2** such that H atoms between the pyrimidines (H1 and H1') are most downfield shifted on dilution or increased temperature.

3.3 Photophysical Properties

The overlaid absorption spectra of **1–3** in chloroform are presented in figure 4-a. The absorption spectra of nonplanar **2** and **3** are markedly similar to that of the fully cyclised N-HSB (**1**) in terms of overall shape. However, their spectra lack the clear fine structure for which the rigidity, planarity and aggregation of **1** are responsible (Gregg *et al.*, 2005). A considerable reduction in ε_{max} due to the loss of a C–C bond fusion that contributes to the π–conjugation (Table 1). Overall the absorption maxima of **2** (304 nm) and **3** (289 nm) are blue-shifted with respect to **1** (354 nm) (Figure 4-a and Table 1). Similarly, the lowest energy bands of **2** (463 nm) and **3** (429 nm) are blue-shifted with respect to **1** (481 nm). These findings are in agreement with the reduction in the degree of conjugation and the depletion of π–electron density in **2** and **3**.

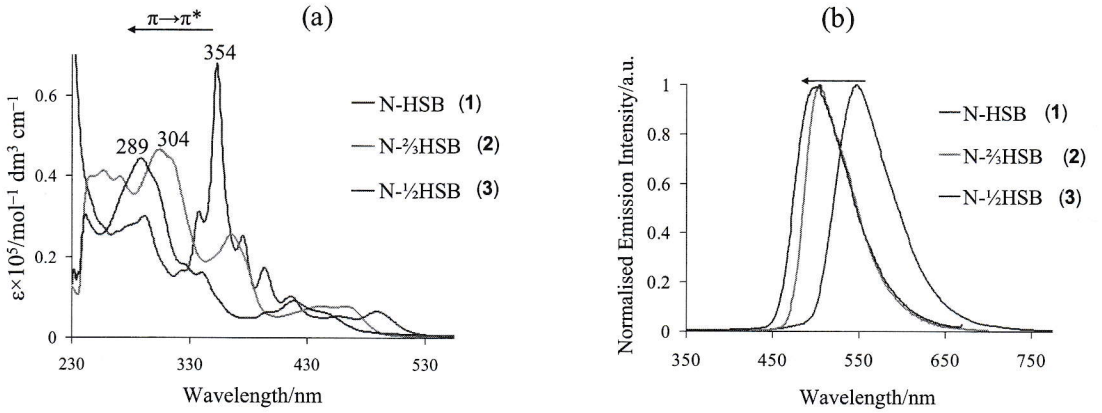

Figure 4. (a) Overlaid absorption spectra and (b) overlaid emission spectra of **1**, **2** and **3** in chloroform at room temperature.

Figure 4-b represents the emission spectra of **1** to **3** in chloroform at room temperature and their λ_{max}^{em} (544, 505 and 502 nm, respectively) have blue-shifted. This is a further consequence of the diminution

in π/π^* framework. Rigidity is known to assist in reducing nonradiative decay and to help prolong excited-state lifetimes (Treadway *et al.*, 1996).

The emission spectra of **1**, **2** and **3** are independent of the wavelength of excitation. The compounds **1**, **2** and **3** in chloroform were excited at all absorption maxima wavelengths with a fixed slit width and in each case the emission maxima remained at 544, 505 and 502 nm, respectively. This further suggests that there is a single luminescent species. The highest intensity emission spectra of **1**, **2** and **3** are generated by irradiating at 354, 304 and 289 nm, which is the λ_{max}^{abs} in the absorption spectrum. Comparison of λ_{max}^{abs} and λ_{max}^{em} of **1**, **2** and **3** is summarized below in table 1.

Table1. Comparison of **1**, **2** and **3** with their λ_{max}^{abs}, λ_{max}^{em} in chloroform

Compound	Structure	λ_{max}^{abs} [nm], ε_{max} [M^{-1} cm^{-1}]	λ_{max}^{em} [nm]
N-HSB (1)	fully cyclized (6 bonds)	354, 68000	544
N-⅔HSB (2)	⅔ cyclized (4 bonds)	304, 46000	505
N-½HSB (3)	half cyclized (3 bonds)	289, 45600	502

The absorption and emission studies of nitrogen-containing aromatic systems show (n,π^*) and (π,π^*) transitions and their nature could be excited singlet state or triplet state. The nature of these excited state transitions varies as singlet or triplet states depending on the molecule's size, shape and the number of heteroatoms it contains and the solvent environment (Bent *et al.*, 1975 and Bandyopadhyay and Harriman, 1977). When additional aromatic rings are added to the nitrogen-containing aromatic system, additional bonding and antibonding levels are introduced resulting in the reduction of the energy of the lowest $\pi \rightarrow \pi^*$ transition (Lee et al., 1999 and Badger and Walker, 1956). Therefore, we expect the lowest excited state transitions of **1**, **2** and **3** are from the (π,π^*) level. This is further supported by the red-shift observed for the emission maxima of **1**, **2** and **3** in polar solvents.

Isolation of **2** and **3** is a step toward a new generation of intensely fluorescing nitrogen-heterosuperbenzenes emitting at a variety of wavelengths. With most well-developed organic polymer and conjugated molecular systems being red to green light emitting materials (Kraft *et al.*, 1998 and Rees *et al.*, 2002), **2** and **3** are important members of the more limited group of compounds that emit in the blue region.

4 Conclusion and Recommendations

In conclusion, the essential steps in the formation of intrinsically nitrogen-doped graphite nanostructures in a controlled and systematic manner have been proven. The presence of N atoms has rendered overall electron-accepting properties to **1** compared to its all-C analogue. The emission studies on **1**, **2** and **3** suggest that the optoelectronic properties of this emerging heterosuperbenzene family will be promising. Synthetic control of the extent and position of N doping such as demonstrated here allows molecular tuning of the optoelectronic properties of the resultant material and

provides the dual advantages of ligand functionality and increased solubility.

Reference

Wu, J., Pisula, W. And Müllen, K. (2007). Graphenes as potential material for electronics. *Chemical Review*, 107(3), 718-747.

Grimsdale, A. C., Chan, K. L., Martin, R. E., Jokisz P. G. And Holmes A. B. (2009). Synthesis of light-emitting conjugated polymers for applications in electroluminescent devices. *Chemical Review*, 109(3), 897-1091.

Aleshin, A., kiebooms, R., Menon, R., Wudle, F. and Heeger, A. J. (1997). Metallic conductivity at low temperatures in poly(3,4-ethylenedioxythiophene) doped with PF_6. *Physical Review B: Condensed Matter and Materials Physics*, 56, 3659.

Müller, S. and Müllen, K. (2007). Expanding benzene to giant graphenes: towards molecular devices. *Philosophiccal Transactions Royal Society A*, 365, 1453-1472.

van de Craats, A. M. and Warman, M. (2001). The core-size effect on the mobility of charge in discotic liquid crystalline materials. *Advanced Materials*, 13(2), 130-133.

Draper, S. M., Gregg, D. J., Schofield, E. R., Brown, W. R., Duati, M., Vos, J. G. and Passaniti, P. (2004). Complexed nitrogen heterosuperbenzene: the coordinating properties of a remarkable ligand. *Journal of the American Chemical Society*, 126(28), 8694-8701.

Rojas, F. M., Rossier, J. F., Brey L., and Palacios J. J. (2008). Performance limits of grapheme-ribbon field-effect transistors. *Physical Review B: Condensed Matter and Materials Physics*, 77, 045301-1-045301-3.

Watson, M. D., Fechtenkotter, A. and Müllen, K. (2001). Big is beautiful-aromaticity revisited from the view point of macromolecular and supramolecular benzene chemistry. *Chemical Review*, 101, 1267-1300.

Hyatt, J. A. (1991). Synthesis of a hexaalkynylhexaphenylbenzene. *Organic Preparation and Procedures International*, 23, 460–463.

Ogliaruso, M. A., Romanelli, M. G. and Becker, E. I. (1965). Chemistry of cyclopentadienones. *Chemical Review,* 65, 261–367.

Iyer, V. S., Wehmeier, M., Brand, J. D., Keegstra, M. A. and Müllen, K. (1997). From Hexa-peri-hexabenzocoronene to "Superacenes". *Angewandte Chemie International Edition*, 36(15), 1604-1607.

Fogel, Y., Kastler, M., Wang, Z., Andrienko, D., Bodwell, G. J. and Müllen, K. (2007). Electron-deficient N-heteroaromatic linkers for the elaboration of large, soluble polycyclic aromatic hydrocarbons and their use in the synthess of some very lasrge transition metal complexes. *Journal of the American Chemical Society*, 129(38), 11743-9.

Lankage, B. S. (2010). Thesis title: *Molecular Materials: N-Doped Graphenes and Their Coordination Complexes*. TCD, University of Dublin.

Wu, J., Fechtenkötter, A., Gauss, J., Watson, M. D., Kastler, M., Fechtenkötter, C., Wagner, M. and Müllen, K. (2004). Controlled self-assembly of hexa-peri-hexabenzocoronenes in solution. *Journal of the American Chemistry Society,* 126, 11311-21.

Ebbesen, T. W. (1997). *Carbon Nanotubes: Preparation and Properties*. CRC Press.

Kraft, A., Grimsdale, A. C. and Holmes, A. B. (1998). Electroluminescent conjugated polymer-seeing polymers in a new light. *Angewandte Chemie International Edition*, 37, 402-428.

Rees, I. D., Robinson, K. L., Holmes, A. B., Towns, C. R. and O'Dell, R. (2002). Recent Developments in light-emitting polymers. *Materials Research Bulletin*, 27, 451-455.

Treadway, J. A., Loeb, B., Lopez, R., Anderson, P. A., Keene, F. R. and Meyer, T. J. (1996). Effect of delocalization and rigidity in the acceptor ligand on MLCT excited-state decay. *Inorganic Chemistry*, 35, 2242-2246.

Draper, S. M., Gregg, D. J. and Madathil, R. (2002). Heterosuperbenzenes: A new family of nitrogen-functionalised, graphitic molecules. *Journal of the American Chemical Society*, 124, 3486-3487.

Gregg, D. J., Bothe, E., Höfer, P., Passaniti, P. and Draper, S. M. (2005). Extending the nitrogen-heterosuperbenzene family: the spectroscopic, redox and photophysical properties of "half-cyclized" N-½HSB and its Ru(II) complex. *Inorganic Chemistry*, 44, 5654-60.

Bent, D. V., Hayon, E. and Moorthy, P. N. (1975). Chemistry of the triplet state of diazines in solution studies by laser spectroscopy. *Journal of the American Chemistry Society*, 97, 5065-5071.

Bandyopadhyay, B. N. and Harriman, A. (1977). Photoreduction of 1,10-phenanthroline. *Journal of the Chemical Scoiety, Faraday Transactions 1*, 73, 663-674.

Lee, S. K., Zu, Y., Herrmann, A., Geerts, Y., Mllen, K. and Bard, A. J. (1999). Electrochemistry, spectroscopy and electrogenerted chemiluminescence of perylene, terrylene and quaterrylene diimides in aprotic solution. *Journal of the American Chemical Society*, 121, 3513-3520.

Badger, G. M. and Walker, I. S. (1956). Polynuclear heterocyclic systems. Part IX n-π*-transitions in the spectra of aromatic aza-hydrocarbons. *Journal of the American Chemical Society*, 122-126.